Green Pathway for Processing Non-mulberry *Antheraea pernyi* Silk Fibroin/Chitin-Based Sponges: Biophysical and Biochemical Characterization

Simone S. Silva [1,2]*, Joana M. Gomes [1,2], Ana Catarina Vale [1,2], Shenzhou Lu [3], Rui L. Reis [1,2,4] and Subhas C. Kundu [1,2]*

[1] 3B's Research Group, I3Bs- Research Institute on Biomaterials, Biodegradables and Biomimetics, University of Minho, Headquarters of the European Institute of Excellence on Tissue Engineering and Regenerative Medicine, AvePark, Parque da Ciência e Tecnologia, Zona Industrial da Gandra, Braga, Portugal, [2] ICVS/3B's- PT Government Associate Laboratory, Braga, Portugal, [3] National Engineering Laboratory for Modern Silk, College of Textile and Clothing Engineering, Soochow University, Suzhou, China, [4] The Discoveries Centre for Regenerative and Precision Medicine, Headquarters at University of Minho, Guimarães, Portugal

Silk protein fibroin (SF)-based matrices from non-mulberry, and mulberry silkworms are used for different applications in regenerative medicine. Silk fiber spun by the wild non-mulberry silkworm *Antheraea pernyi* (Ap) is also a promising biomedical material, due to the presence of the inherent tripeptide sequence of Arginine-Glycine-Aspartic acid (RGD) on the protein fibroin sequences. However, SF derived from the Ap cocoons still lacks exploitation in the healthcare field due to its poor solubility in the conventional solvents. This work addresses the application of green chemistry principles, namely the use of ionic liquids (ILs, 1-butyl-imidazolium acetate) and renewable resources such as *Antheraea pernyi* silk fibroin (ApSF) and chitin (Ch), for the fabrication of sponges from the blends of ApSF and Ch (APC). The formation of β-sheet in different contents during ApSF/Ch/IL was acquired by exposing gels to methanol/water and ethanol/water. The sponges were then obtained by freeze-drying. This approach promotes the formation of both stable and ordered ApSF/Ch-based sponges. The developed sponges show the suitable porosity and interconnectivity, appreciable swelling degree, and tuneable viscoelastic compressive properties for tissue engineering applications. Collectively, the structural properties of these ApSF/Ch-based sponges make them promising candidates for biomedical applications, namely cartilage regeneration.

Keywords: *Antheraea pernyi*, ionic liquids, biomaterials, sponges, chitin, silk fibroin

INTRODUCTION

Silk protein fibroin-based matrices from mulberry silkworms have already shown a broad range of applications in tissue engineering and regenerative medicine due to its versatility, non-toxicity, and biocompatibility as well as their exceptional structural and mechanical properties (Silva et al., 2016; Singh et al., 2016; Woloszyk et al., 2016).

In particular, silk fibroin from the silkworm *Antheraea pernyi* (ApSF) is known to contain a tripeptide sequence of Arginine-Glycine-Aspartic acid (RGD) on the fibroin sequences, which make it a promising biomedical material (Kang et al., 2018; Silva et al., 2019). Despite this value-added and tunable mechanical advantages, the biomedical potential of Ap silk fibroin (ApSF) is underexplored, since ApSF fibers have a strong resistance to chemicals due to its extended antiparallel β-sheet structure and hydrogen bonds among the chains (Zhang et al., 2016; Silva et al., 2019). Ionic liquids (ILs), have emerged as a class of solvents, capable of providing effective platforms to enhance the processability of natural macromolecules (Swatloski et al., 2002; Silva et al., 2012, 2013a, 2017; Chakravarty et al., 2018; Yang et al., 2019). By definition, ILs are known as poorly coordinated salts, liquids at room temperature (Freire et al., 2012; Vekariya, 2017; Gomes et al., 2019). Matrices with different shapes and sizes, e.g., films, hydrogels, sponges, microspheres, have been produced. Their applications as drug delivery systems and tissue regeneration have been investigated (Silva et al., 2013a,b; Singh et al., 2013; Kim et al., 2015; Bendaoud et al., 2017). For instance, chitin, a natural polymer with appealing properties for biomedical applications, presents a high degree of crystallinity and strong hydrogen-bonding, which complicates its processing (Silva et al., 2011, 2013b). Some ILs showed to be able to disrupt the structure of chitin, and dissolve it at concentrations up to 10 wt%, expanding the use of this polymer into a broader range of fields. The ability of ILs to dissolve chitin has enabled its further processing as nanofibers (Barber et al., 2013; Shamshina et al., 2018), microspheres (Silva et al., 2013a), and sponges/porous scaffolds (Silva et al., 2011, 2013b).

As described for the chitin, the silk protein-based matrices were obtained earlier through the dissolution of cocoons from mulberry silkworm, Bombyx mori, non-mulberry silkworms *Antheraea mylitta*, *Samia ricini*, and *Antheraea assamensis* in ILs (Phillips et al., 2004; Silva et al., 2012, 2013, 2016; Goujon et al., 2013; Lozano-Pérez et al., 2014). On these works, the alternative approaches were made by using the ILs particularly for non-mulberries to overcome the restricted uses of fibroins from the silk glands of live silkworms, as their cocoons were insoluble in usual organic solvents used to dissolve mulberry cocoons. The IL platform allowed the fabrication of non-mulberry silk-based hydrogels (Silva et al., 2013) and sponges (Silva et al., 2016) with required properties, namely appreciable swelling degree, suitable porosity and interconnectivity, good mechanical stability and biological performances for tissue engineering applications.

The present work focuses on the creation of green and sustainable strategies for the fabrication of ApSF/Ch-based sponges to be used in biomedical applications in immediate future. To the best of our knowledge, there are no investigations to develop ApSF/Ch-based sponges. Herein, the sponges produced using the green chemistry principles by employing the IL 1-butyl-3-methyl-imidazolium acetate (BMIMAc) as a common solvent to dissolve both the ApSF and Ch. The solutions are further combined to fabricate the blended matrices. The mixtures of the solvents and freezing temperature variations are also applied during the processing to modulate the physical features of the matrices.

MATERIALS AND METHODS

Materials

Chitin from crab shells (Ch; practical grade; Sigma Aldrich) with a degree of N-acetylation of 57.9%, determined by elemental analysis, were ground through a Wiley Mill (model 4, Thomas) and stored in plastic bottles. Ground chitin (106μm) was used throughout the experiments to obtain reproducible results. *Antheraea pernyi* cocoons and fibers were purchased from Mayrin Group Co., Ltd; China. The ionic liquid (IL), 1-butyl-3-methyl imidazolium acetate (BMIMAc) was purchased from Sigma Aldrich (St. Louise USA) and was used as a solvent and used without further purification. All other chemicals were reagent grade and were used as received.

Methods

Degumming Process on Antheraea Pernyi Cocoons

The degumming process was achieved by boiling the 5 g of silk filaments for 1 h in water containing 1.1 g/L of Na_2CO_3, followed by 30 min in water with 0.4 g/L of Na_2CO_3. Finally, the resulting fibroin filaments were extensively rinsed in boiling distilled water and air-dried at room temperature (RT).

Preparation of the Antheraea Pernyi/chitin IL Solutions and Structures Formation

The degummed fibers of Ap were dissolved in BMIMAc at 80°C in a concentration of 2% (w/v). In parallel, chitin powder was also dissolved in BMIMAc at 90°C in a concentration of 1% (w/v). The system was kept under stirring for 2 h (Ap) and 4 h (Ch).

After the dissolution, the solutions were blended in a ratio of 1:1, and they were transferred to cylinder molds, followed by frozen at −80°C and −20°C/−80°C for 2 h. Afterward, the gelation of the blended solutions was acquired by exposing the gels to B—methanol (MeOH): water (80/20), or C- ethanol (EtOH): water (80/20) solution, followed by the IL removal using the same solutions B and C. The non-solvent (EtOH) was changed periodically, and the conductivity of the aliquots was made using a conductivimeter (INOLAB, Multilevel 3) with a SondaWTWTetraCon 325, at room temperature. Then, samples were washed with distilled water and frozen at −80°C, while others were frozen at −20°C for 4 h and at −80°C overnight. Throughout the paper, the chitin/ApSF sponges are referred to as APC80B, APC80C, APC20B, APC20C (see details in **Table 1**).

TABLE 1 | Sample identification used throughout the paper.

Sample identification	Preparation condition	
	Frozen temperature	Solvent gelation
APC80B	−80°C	MeOH: H$_2$O 80/20
APC80C	−80°C	EtOH: H$_2$O 80/20
APC20B	−20°C/−80°C	MeOH: H$_2$O 80/20
APC20C	−20°C/−80°C	EtOH: H$_2$O 80/20

Characterization

FTIR Spectroscopy

The infrared spectra were recorded using a Shimadzu-IR, Prestige 21 spectrometer, in the spectral region of 4,000–650 cm^{-1}, with a resolution of 2 cm^{-1} at 32 scans. The data was acquired using the KBr mode, and, to this end, the samples were powdered, mixed with KBr, and processed into pellets. Fourier self-deconvolution (FSD) of the infrared spectra covering the amide I region (1,595–1,705 cm^{-1}) was performed using the Origin 9.0 Software. To measure the related areas of the amide I components, FSD spectra were curve fitted to Gaussian line shape profiles. The deconvoluted amide I spectra area was normalized, and the relative areas of the single bands were used to determine the fraction of the secondary structural elements. The band assignments and the detailed procedure to determine b-sheet crystallinity were described previously (Hu et al., 2006).

SEM

The different freeze-dried samples were fixed using mutual carbon adhesive tape on aluminum stubs and coated with a conductive gold layer, and their morphology was observed using a NanoSEM-FEI Nova 200 with an integrated microanalysis X-ray system (EDS—energy dispersive spectrometer).

Micro-Computed Tomography (μ-CT)

Non-Destructive characterization of the microstructure of distinct samples was performed through micro-computed tomography (micro-CT) that was performed on a high-resolution device, SkyScan 1272 scan (v1.1.3, Bruker, Boston, USA). The acquisition was conducted under the conditions of intensity 140 μA, a voltage of 71 kV, and a voxel size of 11 μm. The obtained projection images were reconstructed in about 200 slices along the ZZ axis (software NRecon, SkyScan). Then, using the CTAn software (SkyScan), the selected projection images were binarized through a global thresholding (value adjusted to the minimum of the global grayscale histogram from each sample), the reconstructed slice images were processed and through the 3D rendering, the main 3D structural parameters were determined: mean pore size (μm); mean wall thickness (μm); porosity (%); and interconnectivity (%). Finally, the 3D reconstructions were built using CTVox software (version 3.3.0 r1412, Skyscan). At least three samples were analyzed for each condition, and the average value and standard deviation were presented.

Swelling

The swelling tests were performed by immersing the sponges in phosphate buffer solution (PBS) up to 24 h, at 37°C. The weight of the swollen samples was determined after removing the excess surface water by gently tapping the surface with filter paper. The percentage of water uptake was calculated using Equation (1), where W_s is the weight of the swollen sample, and W_d is the weight of the dry sample. Each experiment was repeated three times, and the average value was considered to be the water uptake value.

$$Water\ uptake = \left[\frac{Ws - Wd}{Wd}\right] \times 100 \qquad (1)$$
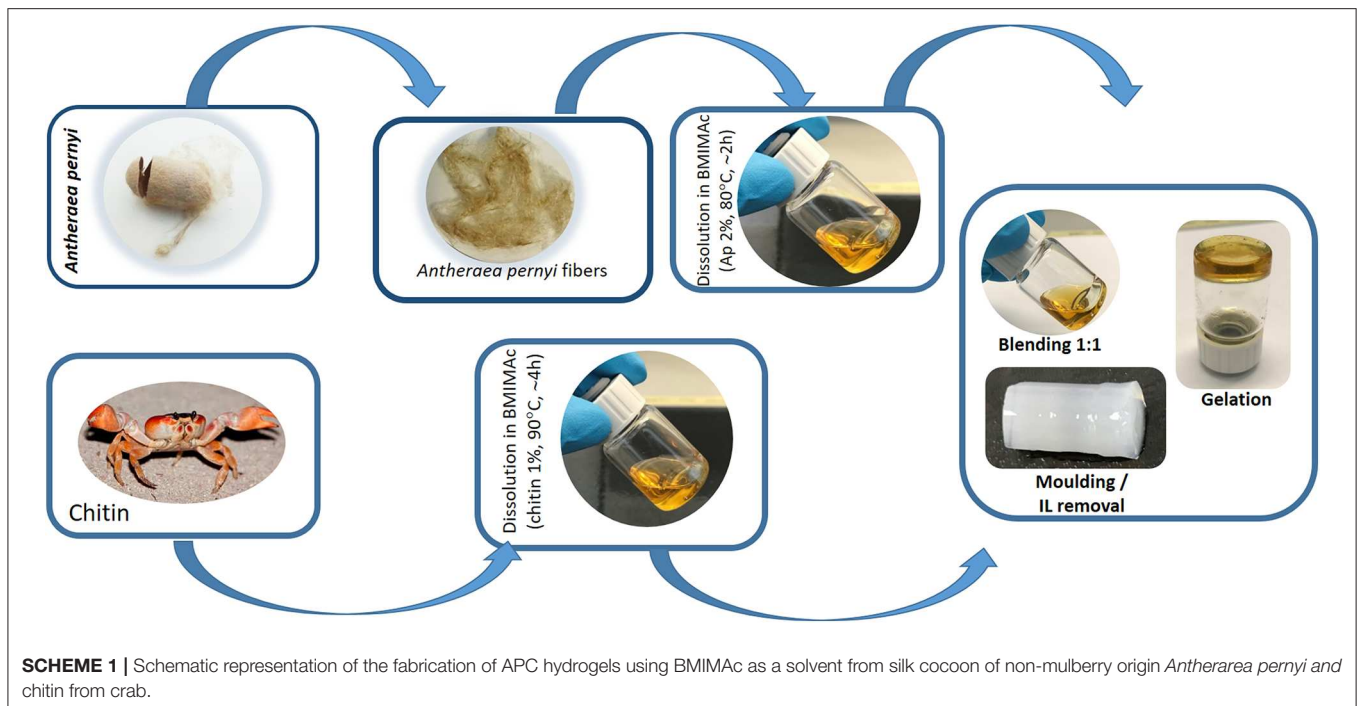
Dynamic Mechanical Analysis (DMA)

Dynamic mechanical analysis was performed using a TRITEC2000B equipment (Triton Technology, UK) equipped with the compressive mode, to evaluate possible alterations on the viscoelastic properties of the developed sponges, when subjected to cyclic loading and immersed in physiologic fluids. Samples were previously soaked in PBS solution up to their equilibration (accordingly to their swelling behavior), and they presented regular geometry, being cylinders with similar dimensions. After equilibration at 37°C, samples were clamped in the DMA apparatus with the total immersion of samples in a reservoir containing PBS solution at 37°C. DMA spectra were obtained using compressive mode cycles of increasing frequency from 0.1 to 20 Hz (5 points per decade) and under constant strain amplitude, corresponding to ~1% of the height of the samples. At least, five samples were tested for each condition, and the average value and standard deviation obtained for storage modulus (E') and loss factor (tan δ) were plotted in function of the loading frequency.

Statistical Analysis

All quantitative experiments were run in triplicate, and the results are expressed as means ± standard deviation for $n = 3$, and $n = 5$ for the DMA analysis. Statistical analysis of the data was conducted by two-way ANOVA with Bonferroni's post-test using GraphPadPrism v. 8.0 for Windows (GraphPad Software, San Diego, http://www.graphpad.com). Differences between the groups at $p \leq 0.05$ were considered to be statistically significant.

RESULTS AND DISCUSSION

Efficient dissolution and processing of both *Antherarea pernyi* silk fibroin (ApSF) and chitin (Ch) were reached using BMIMAc at concentrations of 2 and 1% (w/v), respectively. Both solutions were yellow and viscous (**Scheme 1**), and they also showed excellent stability (1–2 weeks in an inert atmosphere). Previous studies, made in our laboratory, revealed that ApSF/BMIMAc gels at a concentration below 5% (w/v) were fragile (data not shown). However, ApSF/BMIMAc solution combined with chitin/BMIMAc at low concentration (1% w/v), resulted in APC/BMIMAc gels with good mechanical stability. The preparation of the APC matrices was achieved, as depicted in (**Scheme 1**). Earlier studies described that strategies involving combinations of proteins and polysaccharides could be used to process matrices that may mimic the naturally occurring environment of certain tissues (Silva et al., 2008; Singh et al., 2016; Rosellini et al., 2018). Following these research lines, ApSF and chitin are excellent natural raw materials for the design of porous matrices with potential advantages in terms of chemistry versatility, biocompatibility, and controlled degradability. By its turn, similar to *Bomby mori* SF, *Antheraea pernyi* SF has broad applicability mainly due to the presence of Arg-Gly-Asp (RGD) peptide sequences, which promote cell adhesion and proliferation in ApSF filaments from which the sericin coating has been removed by degumming (Silva et al., 2019). However, the degummed fibers have a lack of solubility in common solvents like lithium bromide, probably due to strong hydrogen bonding.

SCHEME 1 | Schematic representation of the fabrication of APC hydrogels using BMIMAc as a solvent from silk cocoon of non-mulberry origin *Antherarea pernyi and* chitin from crab.
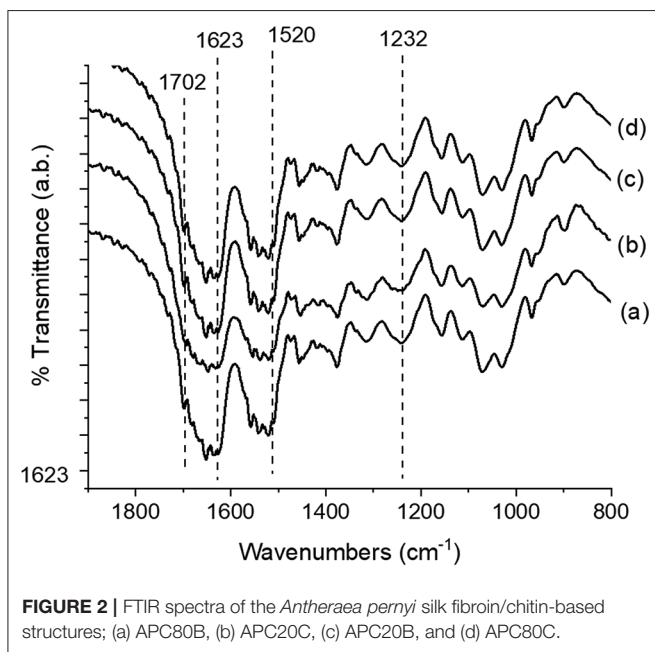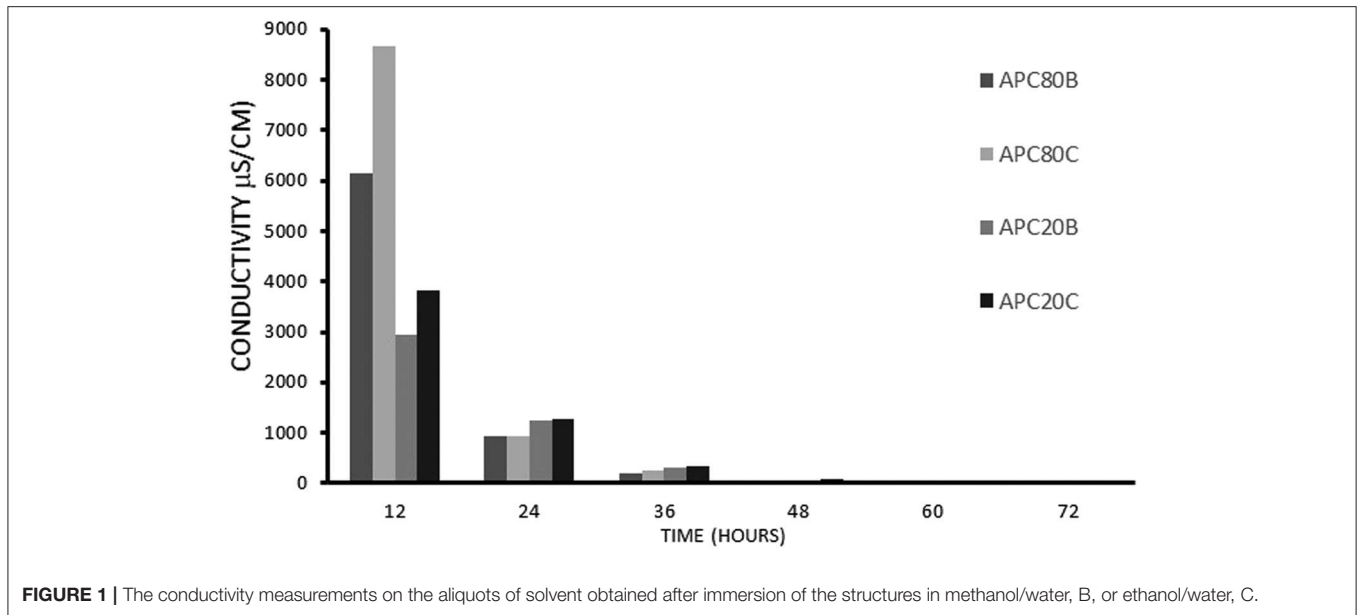
In this sense, some ILs such as BMIMAc, have emerged as a suitable solvent not only for mulberry SF but also for non-mulberry SF ones like Eri silk, *Samia/Philosamia ricini*, tropical tasar, *Antheraea mylitta* (Silva et al., 2013, 2016). However, to date, the use of BMIMAc in the dissolution of ApSF cocoons is still limited. On the other hand, the processability of natural polymers such as chitin, chitosan, cellulose, and agarose in different shapes has been successfully described (Tejwant et al., 2010; Silva et al., 2011, 2013a,b; Barber et al., 2013; Nunes et al., 2017), expanding their potential uses in biomedical field.

Upon cooling, both viscous APC/IL solutions resulted in the formation of gels (ionogels), which were molded into a cylindrical shape. Similar behavior was also observed in previous studies during the cooling of the Eri silkworm, *Samia i ricini* SF/BMIMAc solutions (Silva et al., 2016). By definition, in an ionogel, the IL is immobilized in a pathway that involves the formation of a 3D network that is responsible for the solid-like behavior of the matrices (Néouze et al., 2006; Le Bideau et al., 2011). Methanol/ethanol solutions or even ethanol vapor were often used to induce the β-sheet content through structural rearrangement of chains to form covalent bonds (Silva et al., 2016); thus, we hypothesized that the immersion of the APC/IL gels not only in MeOH:H$_2$O (solvent B) and EtOH:H$_2$O (solvent C) would provide valuable paths for β-sheet formations and also tune the properties of the resulting materials. Our results demonstrated that the samples treated with solvent B produced architectures with good mechanical stability, while those treated with solvent C were weaker when compared to others treated with solvent B. As mentioned before, these findings could be associated with β-sheet formations, which are discussed in the later sections.

Several toxicity assays have proved that some commonly used ILs exhibit toxicity (Gomes et al., 2019). With this in mind, the use of an IL in the fabrication of a biomaterial demands its removal from the final product. Taking into account that BMIMAc, IL, has inherent high conductivity, the monitoring of IL removal was carried out through conductivity measurements during the immersion of the gels into solvent B and C for 3 days. (**Figure 1**) shows the progressive decrease in conductivity during the IL removal process. The samples were assumed to be completely free from the BMIMAc when the conductivity of the aliquots was below 1.5 μS/cm. This finding suggests that the produced gels have a low level of toxicity, as evidenced in other studies, including cell culture (Silva et al., 2016).

All the samples exhibited peaks centered at 1,221, 1,521, and 1,667 cm^{-1}, corresponding to amide I, II, and III, respectively (**Figure 2**). These peaks constitute the typical random coil conformation. After dissolution/processability and stabilization treatment using MeOH: H$_2$0 (solvent B) and EtOH: H$_2$O (solvent C), the APC samples showed peaks at 1,624–1,621 cm^{-1} (amide I) and 1,521 cm^{-1} (amide II); which are related to intermolecular β-sheet bands (Um et al., 2001). The absence of the characteristic peaks of BMIMAC (Silva et al., 2016) indicated that this solvent was eliminated from the structures. Therefore, the observed structural features of the APC samples revealed that the use of BMIMAc did not affect the typical β-sheet formation induced by stabilization treatment.

By analyzing the curve fitting of the FTIR spectra (data not shown) of the amide I region between 1,595 and 1,705 cm^{-1} for all APC samples, and taking into account that the regions of 1,600–1,640 cm^{-1} and 1,690–1,705 cm^{-1} were associated with intermolecular β-sheet bands (Um et al., 2001; Silva et al.,

FIGURE 1 | The conductivity measurements on the aliquots of solvent obtained after immersion of the structures in methanol/water, B, or ethanol/water, C.

FIGURE 2 | FTIR spectra of the *Antheraea pernyi* silk fibroin/chitin-based structures; (a) APC80B, (b) APC20C, (c) APC20B, and (d) APC80C.

2016), the amount of secondary structure in APC samples was determined. The β-sheet content found for APC samples was: 38.03% (APC80B), 42.69% (APC80C), 20.82% (APC20B), and 17.89% (APC20C). These findings suggest that the gelation temperature step and the use of different solvents influenced the β-sheet content on the different contents.

All APC gels were freeze-dried to produce sponges, whose morphologies were investigated by SEM (see **Figure 3**). By analyzing the morphology of the cross-sections of the produced APC sponges (**Figure 3**), it was possible to verify that all samples have an open structure with pore sizes between 100 and 150 μm, independently of the solvent used in the stabilization step. Also, a

quantitative analysis of the 3D morphometric parameters of the produced sponges was performed by micro-CT analysis. The 3D images of the scaffolds obtained from digital geometry processing from a series of two-dimensional X-ray images are illustrated (**Figure 4**). Through these images, the mean pore size, mean wall thickness, porosity, interconnectivity were quantified (**Table 1**). The data revealed that the APC-based sponges have pore sizes ranging between 95 and 137 μm, while the porosity values were between 86 and 88%, and interconnectivity values range from 75 to 88%. It seems that the different freezing temperatures used could explain the morphological variations observed in the samples. Comparing the morphological features of the earlier developed APC-based sponges with similar studies where BMIMAc was used to dissolution/processing of non-mulberry Eri silk (*Samia/Philosamia ricini*) into sponges (Silva et al., 2016); we conclude that the porosity and interconnectivity values found for APC-based sponges are superior. Those developed structures exhibited porosity, pore size, and interconnectivity that may allow not only the successful seeding of cells but also their proliferation into the developed structures.

Swelling Behavior

The swelling degree of the developed sponges after immersing in PBS at 37°C (**Figure 5**). All the sponges have considerable swelling degrees (up to 900% after 24 h), probably due to their high porosities (from 86.4 to 89.1%). Moreover, all APC-based sponges were able to keep their stability along with the assay, which is in accordance with the already published data stating that the stability of the structures was strongly associated with the β-sheet crystalline contents (Silva et al., 2016). However, no statistical differences were observed among the different time points at the four different conditions. In the same condition, there were also no significant differences among the different time points.

DMA experiments were performed to evaluate the variations of the viscoelastic properties of the sponges under compressive
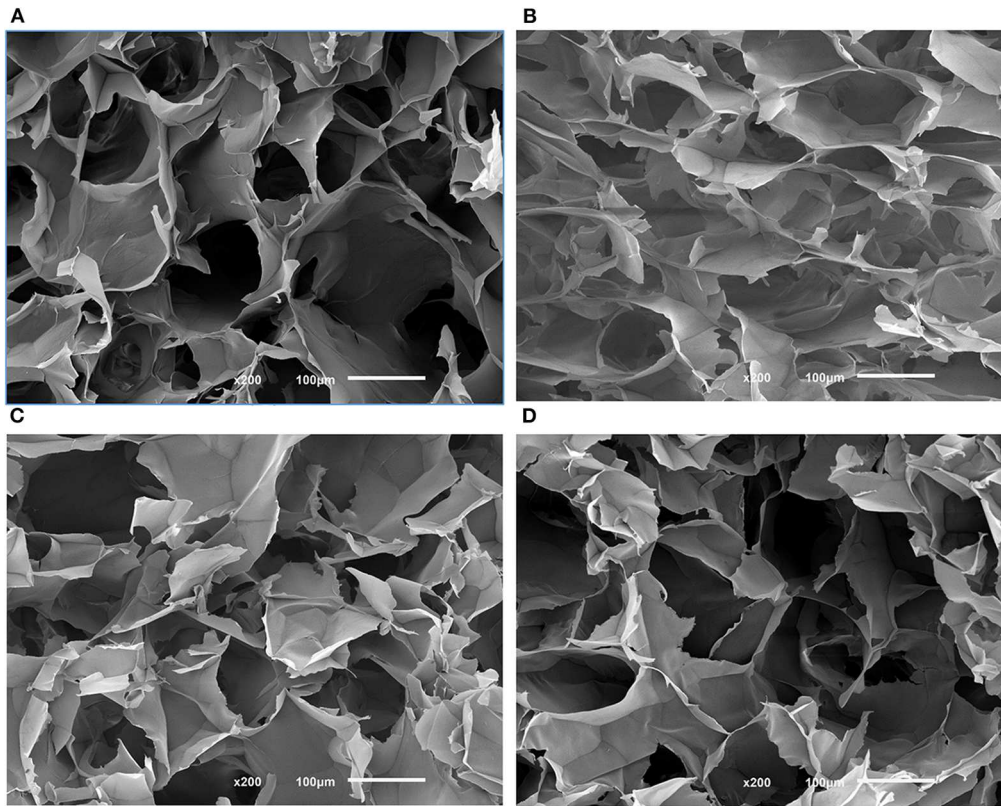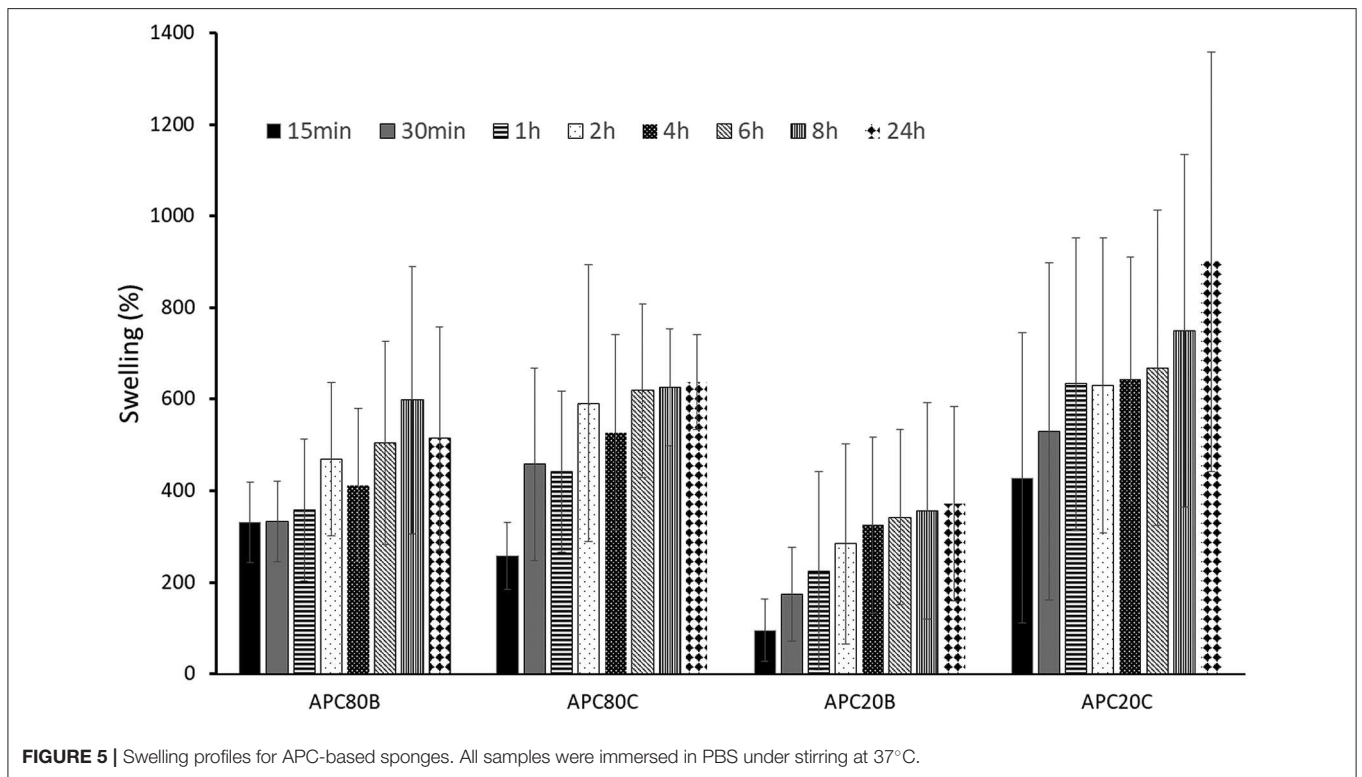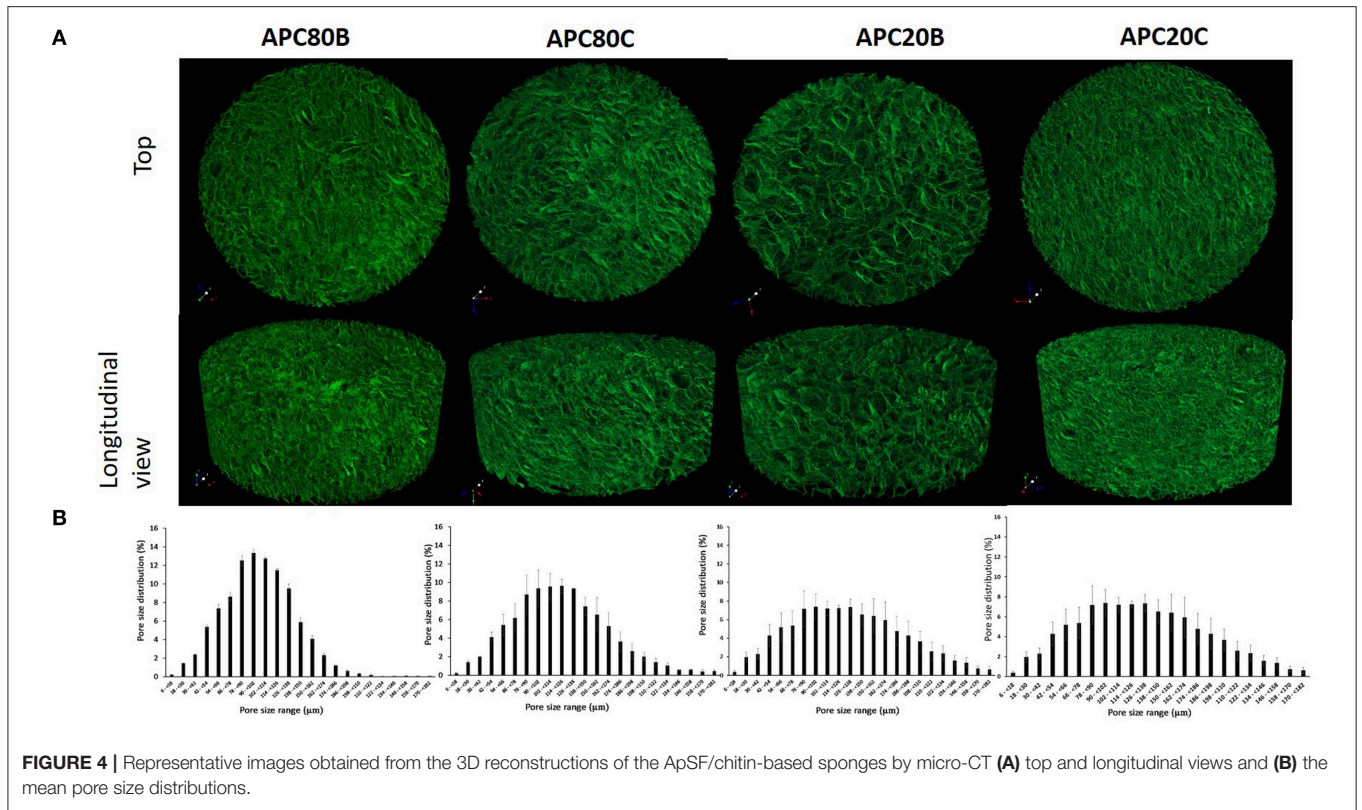
FIGURE 3 | Morphological features of different SEM images of the cross-sections of the APC80B **(A)**, APC80C **(B)**, APC20B **(C)**, and APC20C **(D)** scaffolds. Scale bars represent 100 μm.

loading and immersed in PBS solution at 37°C, trying to simulate the physiological environment (**Figure 6**). Variations of both storage modulus (E') and loss factor (tan δ) during frequency scans are shown in (**Figure 5**). Besides, (**Tables 2**, **3**) summarized the viscoelastic properties obtained at a physiological frequency (1 Hz). These DMA results showed a small increase in E' with the increasing frequency for all samples, varying between 70 and 110 kPa for APC80B and APC 80C, and between 50 and 70 kPa for APC 20B and APC 20C. The results indicated that the mechanical properties of the APC sponges could be modulated by the formation of an organized structure, richer in β-sheet content. Moreover, studies on silk fibroin-based scaffolds described the β-sheet formation as a critical factor that determines the mechanical properties of any particular SF (Silva et al., 2013, 2016). Therefore, it seems that the differences in β-sheet content within the matrices, determined by the deconvolution of the FTIR spectra of the samples, could be useful to modulate the storage modulus of the samples. In fact, the highest β-sheet content, calculated for APC80B (38.03%) and APC80C (42.69%), may have a significant role in the formation of a more rigid network, evidenced by their highest storage modulus (**Table 2**). In a similar study, higher E'(range of 233-797 kPa) were found in non-mulberry Eri silk-based sponges (Silva et al., 2016). The differences between the studies could be associated with the

preparation conditions, which in turn affected the porosity and β-sheet content on silk-based matrices. Regarding the variation of the tan δ, for all sponges, it was observed a slight increase with the frequency increasing, evidencing that these materials became viscous and less elastic, and presenting more ability to dissipate energy. However, since the loss factor values were lower than 1, it should be assumed that all sponges can recover due to their higher elastic component.

CONCLUSIONS

The present work provides an innovative and sustainable strategy to produce blended sponges composed of silk protein fibroin derived from *Antheraea pernyi* cocoons and chitin from crab shells. Moreover, the structural features of the developed structures such as the differences in β-sheet contents, suitable porosity, interconnectivity, appreciable swelling degree, and tuneable viscoelastic compressive properties suggest that they can be good candidates for tissue engineering approaches. The formation of ApSF/chitin/BMIMAc gels also demonstrated to be flexible, which allows adapting the shape of the resulting matrices according to the defect sites where it would be implanted for tissue regenerations. In the immediate future, *in vitro* biological performance tests of the sponges with primary
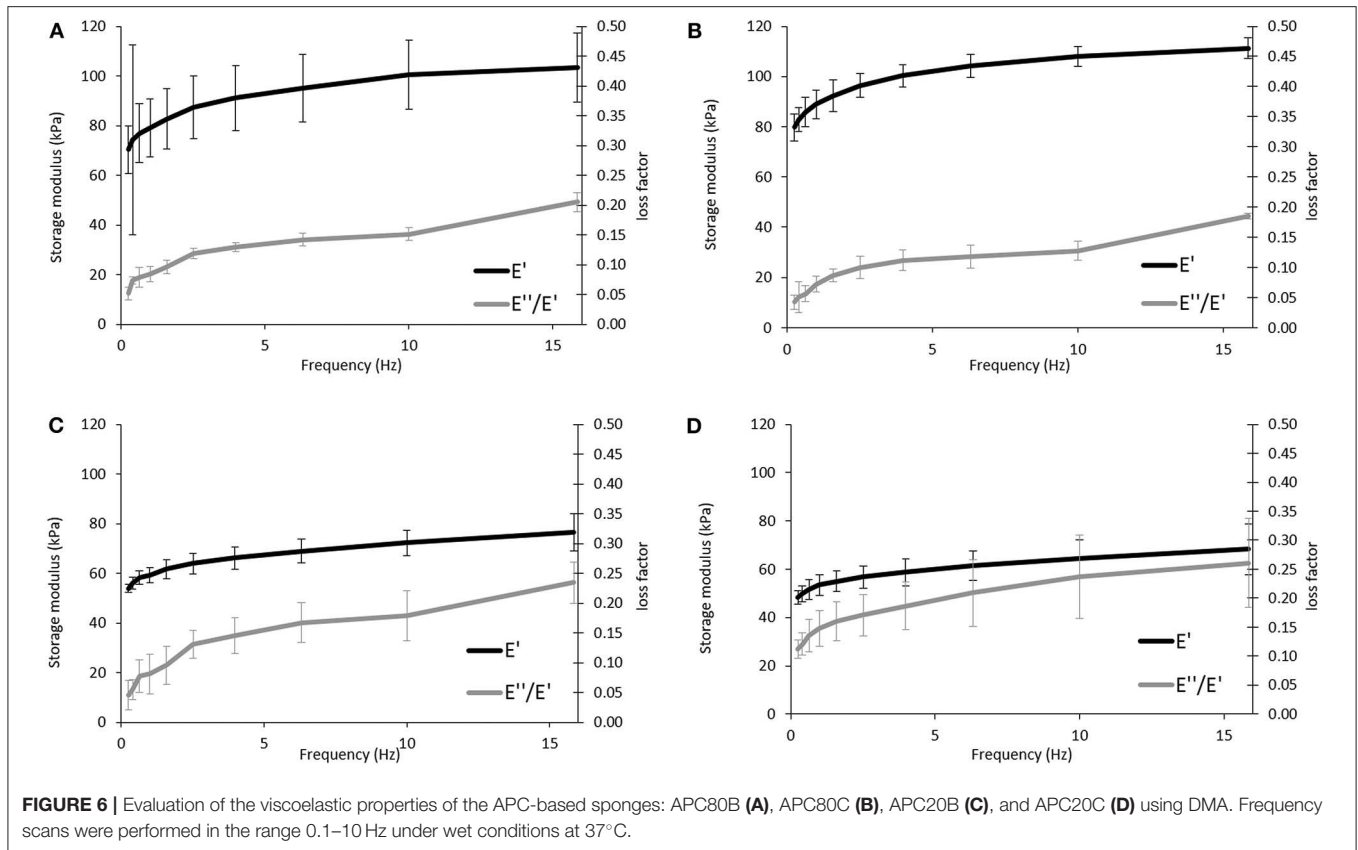
FIGURE 4 | Representative images obtained from the 3D reconstructions of the ApSF/chitin-based sponges by micro-CT **(A)** top and longitudinal views and **(B)** the mean pore size distributions.

FIGURE 5 | Swelling profiles for APC-based sponges. All samples were immersed in PBS under stirring at 37°C.

FIGURE 6 | Evaluation of the viscoelastic properties of the APC-based sponges: APC80B **(A)**, APC80C **(B)**, APC20B **(C)**, and APC20C **(D)** using DMA. Frequency scans were performed in the range 0.1–10 Hz under wet conditions at 37°C.

TABLE 2 | Microstructural features of the APC-based sponges obtained by micro-CT.

Sample	Mean pore size (μm)	Thickness (μm)	Porosity (%)	Interconnnectivity (%)
APC80B	101.82 ± 1.64	14.80 ± 0.05	88.39 ± 0.43	86.81 ± 3.54
APC80C	124.13 ± 15.13	15.04 ± 0.38	89.17 ± 0.99	88.20 ± 5.17
APC20B	137.55 ± 8.36	15.12 ± 0.43	88.77 ± 1.03	75.93 ± 4.62
APC20C	110.41 ± 6.18	14.33 ± 0.06	86.46 ± 5.07	88.57 ± 4.13

TABLE 3 | Viscoelastic properties of the APC based-sponges under compressive loading at a physiological frequency (1 Hz).

Sample	Storage modulus (kPa)	tanδ
APC80B	79.01 ± 11.8	0.08 ± 0.01
APC80C	88.91 ± 5.7	0.07 ± 0.01
APC20B	59.3 ± 3.11	0.08 ± 0.03
APC20C	53.4 ± 4.24	0.15 ± 0.03

cells will be performed to elucidate the biological behavior of the APC-based sponges. This strategy allows overcoming the limited use of silk fibroin from *Antheraea pernyi* cocoons as 3D-based structures, which open the prospects for its use for biomedical applications.

DATA AVAILABILITY STATEMENT

The datasets generated for this study are available on request to the corresponding author.

AUTHOR CONTRIBUTIONS

Each author played a major role in the development of the work and writing the manuscript. RR and SK supervised the work. SS (an Assistant Researcher) and JG (Ph.D. student) were involved in all aspects of experimentation and have contributed equally to this manuscript. AV is is a Junior researcher who undertook the DMA work. SL provided the silk of *Antheraea pernyi* and contributed to the experiments and discussion of the manuscript.

FUNDING

REFERENCES

Barber, P. S., Griggs, C. S., Bonner, J. R., and Rogers, R. D. (2013). Electrospinning of chitin nanofibers directly from an ionic liquid extract of shrimp shells. *Green Chem.* 15, 601–607. doi: 10.1039/c2gc36582k

Bendaoud, A., Maigret, J. E., Leroy, E., Cathala, B., and Lourdin, D. (2017). Cellulose-xyloglucan composite film processing using ionic liquids as co-solvents. *AIP Conf. Proc.* 1914:070008. doi: 10.1063/1.5016735

Chakravarty, J., Rabbi, M. F., Bach, N., Chalivendra, V., Yang, C.-L., and Brigham, C. J. (2018). Fabrication of porous chitin membrane using ionic liquid and subsequent characterization and modelling studies. *Carbohydr. Polym.* 198, 443–451. doi: 10.1016/j.carbpol.2018.06.101

Freire, M. G., Cláudio, A. F. M., Araújo, J. M. M., Coutinho, J. A. P., Marrucho, I. M., Lopes, J. N. C., et al. (2012). Aqueous biphasic systems: a boost brought about by using ionic liquids. *Chem. Soc. Rev.* 41, 4966–4995. doi: 10.1039/c2cs35151j

Gomes, J. M., Silva, S. S., and Reis, R. L. (2019). Biocompatible ionic liquids: fundamental behaviours and applications. *Chem. Soc. Rev.* 48, 4317–4335. doi: 10.1039/C9CS00016J

Goujon, N., Rajkhowa, R., Wang, X., and Byrne, N. (2013). Effect of solvent on ionic liquid dissolved regenerated antheraea assamensis silk fibroin. *J. Appl. Poly. Sci.* 128, 4411–4416. doi: 10.1002/app.38666

Hu, X., Kaplan, D., and Cebe, P. (2006). Determining beta-sheet crystallinity in fibrous proteins by thermal analysis and infrared spectroscopy. *Macromolecules* 39, 6161–6170. doi: 10.1021/ma0610109

Kang, Z., Wang, Y., Xu, J., Song, G., Ding, M., Zhao, H., et al. (2018). An RGD-containing peptide derived from wild silkworm silk fibroin promotes cell adhesion and spreading. *Polymers* 10, 1193–1205. doi: 10.3390/polym10111193

Kim, S. Y., Hwang, J.-Y., Seo, J.-W., and Shin, U. (2015). Production of CNT-taxol-embedded PCL microspheres using an ammonium-based room temperature ionic liquid: as a sustained drug delivery system. *J. Colloid Interface Sci.* 442, 147–153. doi: 10.1016/j.jcis.2014.11.044

Le Bideau, J., Viau, L., and Vioux, A. (2011). Ionogels, ionic liquid based hybrid materials. *Chem. Soc. Rev.* 40, 907–925. doi: 10.1039/C0CS00059K

Lozano-Pérez, A., Montalbán, M. G., Aznar-Cervantes, S., Cragnolini, F., Cenis, J., and Víllora, G. (2014). Production of silk fibroin nanoparticles using ionic liquids and high-power ultrasounds. *J. Appl. Poly. Sci.* 132, 41702–41710. doi: 10.1002/app.41702

Néouze, M.-A., Le Bideau, J., Gaveau, P., Bellayer, S., and Vioux, A. (2006). Ionogels, new materials arising from the confinement of ionic liquids within silica-derived networks. *Chem. Mater.* 18, 3931–3936. doi: 10.1021/cm060656c

Nunes, C. S., Rufato, K. B., Souza, P., de Almeida, E. A. M. S., da Silva, M. J. V., Scariot, D. B., et al. (2017). Chitosan/chondroitin sulfate hydrogels prepared in [Hmim][HSO4] ionic liquid. *Carbohydr. Polym.* 170, 99–106. doi: 10.1016/j.carbpol.2017.04.073

Phillips, D. M., Drummy, L. F., Conrady, D. G., Fox, D. M., Naik, R. R., Stone, M. O., et al. (2004). Dissolution and regeneration of bombyx mori silk fibroin using ionic liquids. *J. Am. Chem. Soc.* 126, 14350–14351. doi: 10.1021/ja046079f

Rosellini, E., Zhang, Y. S., Migliori, B., Barbani, N., Lazzeri, L., Shin, S. R., et al. (2018). Protein/polysaccharide-based scaffolds mimicking native extracellular matrix for cardiac tissue engineering applications. *J. Biomed. Mater. Res. A* 106, 769–781. doi: 10.1002/jbm.a.36272

Shamshina, J. L., Zavgorodnya, O., Choudhary, H., Frye, B., Newbury, N., and Rogers, R. D. (2018). In search of stronger/cheaper chitin nanofibers through electrospinning of chitin–cellulose composites using an ionic liquid platform. *ACS Sustain. Chem. Eng.* 6, 14713–14722. doi: 10.1021/acssuschemeng.8b03269

Silva, S. S., Duarte, A., Oliveira, J., Mano, J. F., and Reis, R. L. (2013b). Alternative methodology for chitin–hydroxyapatite composites using ionic liquids and supercritical fluid technology. *J. Bioact. Compat. Pol.* 28, 481–491. doi: 10.1177/0883911513501595

Silva, S. S., Duarte, A. R. C., Carvalho, A. P., Mano, J. F., and Reis, R. L. (2011). Green processing of porous chitin structures for biomedical applications combining ionic liquids and supercritical fluid technology. *Acta Biomater.* 7, 1166–1172. doi: 10.1016/j.actbio.2010.09.041

Silva, S. S., Duarte, A. R. C., Mano, J. F., and Reis, R. L. (2013a). Design and functionalization of chitin-based microsphere scaffolds. *Green Chem.* 15, 3252–3258. doi: 10.1039/c3gc41060a

Silva, S. S., Kundu, B., Lu, S., Reis, R. L., and Kundu, S. C. (2019). Chinese oak tasar silkworm antheraea pernyi silk proteins: current strategies and future perspectives for biomedical applications. *Macromol. Biosci.* 19:1800252. doi: 10.1002/mabi.201800252

Silva, S. S., Mano, J. F., and Reis, R. L. (2017). Ionic liquids in the processing and chemical modification of chitin and chitosan for biomedical applications. *Green Chem.* 19, 1208–1220. doi: 10.1039/C6GC02827F

Silva, S. S., Motta, A., Rodrigues, M. T., Pinheiro, A. F. M., Gomes, M., Mano, J. F., et al. (2008). Novel genipin-cross-linked chitosan/silk fibroin sponges for cartilage engineering strategies. *Biomacromolecules* 9, 2764–2774. doi: 10.1021/bm800874q

Silva, S. S., Oliveira, N. M., Oliveira, M. B., da Costa, D. P. S., Naskar, D., Mano, J. F., et al. (2016). Fabrication and characterization of Eri silk fibers-based sponges for biomedical application. *Acta Biomater.* 32, 178–189. doi: 10.1016/j.actbio.2016.01.003

Silva, S. S., Popa, E., Gomes, M., Oliveira, M., Nayak, S., Subia, B., et al. (2013). Silk hydrogels from non-mulberry and mulberry silkworm cocoons processed with ionic liquids. *Acta Biomater.* 9, 8972–8982. doi: 10.1016/j.actbio.2013.06.044

Silva, S. S., Santos, T., Cerqueira, M. T., Marques, A. P., Reys, L. L., Silva, T. H., et al. (2012). The use of ionic liquids in the processing of chitosan/silk hydrogels for biomedical applications. *Green Chem.* 14, 1463–1470. doi: 10.1039/c2gc16535j

Singh, N., Koziol, K. K., Chen, J., Patil, A. J., Gilman, J., Trulove, P., et al. (2013). Ionic liquids-based processing of electrically conducting chitin nanocomposite scaffolds for stem cell growth. *Green Chem.* 15, 1192–1202. doi: 10.1039/c3gc37087a

Singh, Y., Bhardwaj, N., and Mandal, B. (2016). Potential of agarose/silk fibroin blended hydrogel for *in vitro* cartilage tissue engineering. *ACS Appl. Mater. Interfaces* 8, 21236–21249. doi: 10.1021/acsami.6b08285

Swatloski, R., Spear, S., Holbrey, J., and Rogers, R. (2002). Dissolution of cellose with ionic liquids. *J. Am. Chem. Soc.* 124, 4974–4975. doi: 10.1021/ja025790m

Tejwant, S., Trivedi,. J. T., and Kumar, A. (2010). Dissolution, regeneration and ion-gel formation of agarose in room-temperature ionic liquids. *Green Chem.* 12, 1029–1035. doi: 10.1039/b927589d

Um, I., Kweon, H., Park, Y., and Hudson, S. (2001). Structural characteristics and properties of the regenerated silk fibroin prepared from formic acid. *Int. J. Biol. Macromol.* 29, 91–97. doi: 10.1016/S0141-8130(01)00159-3

Vekariya, R. (2017). A review of ionic liquids: applications towards catalytic organic transformations. *J. Mol. Liqu.* 227, 44–60. doi: 10.1016/j.molliq.2016.11.123

Woloszyk, A., Buschmann, J., Waschkies, C., Stadlinger, B., and Mitsiadis, T. (2016). Human dental pulp stem cells and gingival fibroblasts seeded into silk fibroin scaffolds have the same ability in attracting vessels. *Front. Physiol.* 7, 140–147. doi: 10.3389/fphys.2016.00140

Yang, Y. J., Ganbat, D., Aramwit, P., Bucciarelli, A., Chen, J., Migliaresi, C., et al. (2019). Processing keratin from camel hair and cashmere with ionic liquids. *Express Polym. Lett.* 13, 97–108. doi: 10.3144/expresspolymlett.2019.10

Zhang, C., Chen, X., and Shao, Z. (2016). Sol–gel transition of regenerated silk fibroins in ionic liquid/water mixtures. *ACS Biomater. Sci. Eng.* 2, 12–18. doi: 10.1021/acsbiomaterials.5b00149